

## Expression of chirality in deuterated benzene-1,3,5-tricarboxamides

Jeffrey C. Everts, Seda Cantekin<sup>[a]</sup>, Paul van der Schoot<sup>[b]</sup>, Anja R. A. Palmans<sup>\*,[a]</sup>

**Abstract:** *N,N',N''*-trialkylated-benzene-1,3,5-tricarboxamides (BTAs) form helical supramolecular polymers, which are inherently chiral objects. A preference for the formation of a right-handed or left-handed helix is observed, if deuterium is used for the formation of a stereocenter. The net helicity is measured with CD spectroscopy, while the fraction polymerized material can be measured with UV-VIS

spectroscopy. Here, we report a competing nucleated self-assembly model in order to describe the net helicity and fraction polymerized material as function of temperature in deuterated benzenetricarboxamides (D-BTAs). The model discussed in this work is able to predict these quantities for a dilute solution in dodecane in a certain temperature regime. However, a good prediction is not possible at low

temperatures or in solvent mixtures of heptane with methylcyclohexane (MCH) or iso-octane. This suggests that solvent molecules play an active role in the self-assembly process.

**Keywords:** ((self-assembly · synthesis · CD · helicity · chirality))

### Introduction

Molecular chirality plays an important role in organic chemistry ever since Van't Hoff proposed the concept of a tetrahedral carbon<sup>[1]</sup>. Consequently, two molecules consisting of the same bonds between various atoms are not necessarily equal, since the spatial arrangement of the various chemical groups may differ. The field of stereochemistry that could develop after this discovery gave rise to the development of chemical structures with the presence of many beautiful forms of chirality, such as axial chirality, planar chirality or chirality due to atropisomerism. Still, the most well known form of chirality in organic chemistry is chirality due to the presence of a stereocenter, such that the molecule is asymmetric.

At a first glance, only molecular chirality is thoroughly discussed in basic (organic) chemistry text books. However, chirality in chemical compounds does not need to be restricted to the molecular scale. A well-known example is the  $\alpha$ -helical structure in proteins. This structure is chiral due to its shape, since a helix cannot be superimposed on its mirror image. We can even go to larger

length scales than this: the supramolecular polymer F-actin is also chiral<sup>[2]</sup>, again due to a helical conformation. Interestingly, a hierarchy of chirality can be seen in this protein: F-actin as a whole is a helix, the monomeric building blocks of this polymer, the globular protein G-actin, contain many  $\alpha$ -helical substructures and G-actin itself consists of amino acids which are chiral due to the presence of stereocenters (with of course the exception of glycine).

The presence of chirality on a larger length scale is also investigated in synthetic molecules. A notable example is that of deuterated polyisocyanates by Green *et al* <sup>[3]</sup>. By deuteration of the monomeric building blocks, unexpected high optical activities were measured for this covalent helical polymer in solution. This was attributed to the presence of a stereocenter that gave rise to the formation of almost exclusively one of the two types of helices. It can be said that in this system chirality is transferred from a molecular scale to the mesoscopic scale of the polymer. Green explained this effect induced by a simple deuteration with the difference in the zero-point vibrational energy of the C-H bond as compared to the C-D bond.

This type of chirality transfer was even observed in our group for many supramolecular polymers such as in oligo(*p*-phenylenevinylene) derivatives (OPVs) <sup>[4]</sup> and in methyl substituted *N,N',N''*-trialkylated-benzene-1,3,5-tricarboxamides (methylated BTAs) <sup>[5,6]</sup>. BTAs are interesting molecules because of their simple chemical structure, which accommodates the formation of quasi-one dimensional helical aggregates via threefold intermolecular hydrogen bonding<sup>[5,6]</sup>. In contrast to the system of Green, the preference for one of the two helical senses in methylated

[a] Laboratory of Macromolecular and Organic Chemistry  
Eindhoven University of Technology  
PO Box 513, 5600 MB Eindhoven, The Netherlands  
Fax: (+)31402451036  
E-mail: E.W.Meijer@tue.nl / a.palmans@tue.nl

[b] Theory of Polymers and Soft Matter Group  
Eindhoven University of Technology  
PO Box 513, 5600 MB Eindhoven, The Netherlands

BTAs can be the result of steric interactions, since the residual group that forms the stereocenter is reasonable large.

of Oosawa and Kasai, which allows a competition of formation between two active species, we hope to get more insights in the y (Figure 1).

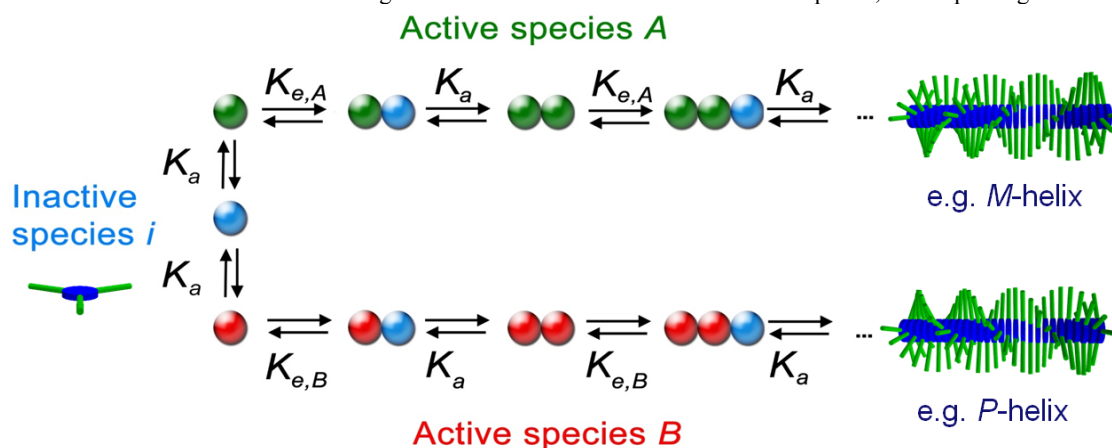
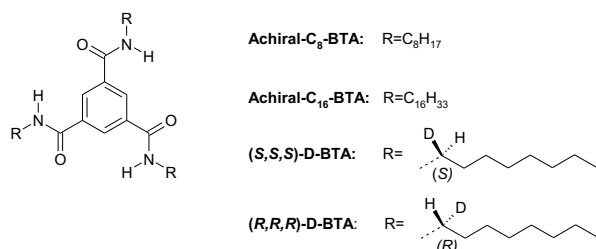


**Figure 1.** Graphical representation of the competing nucleated self-assembly model. Monomeric units need to be activated in order to attach to a growing supramolecular polymer chain. Monomers can bind to two different types of polymers indicated by *A* and *B*, which in our case denote two different helical senses of a stack. The activation of an inactive species is governed by an equilibrium constant  $K_a$ , while the growth of a polymeric chain is governed by an elongation constant  $K_{e\alpha}$  ( $\alpha = A, B$ ).

However, the effect of deuteration in a supramolecular polymer has not been investigated. This motivated us to introduce chirality in a BTA molecule by a deuteration of the three alkyl chains. This work was done by Seda Cantekin and Dirk Balkenende, which synthesized the two enantiomers for a symmetric deuterated BTA (Scheme 1). The synthesis will be reported elsewhere<sup>[7]</sup>.

Notable for the D-BTAs is that the cooling curves obtained by temperature dependent CD spectroscopy show an almost linear dependence in certain temperature regimes, in contrast to their methylated analogues<sup>[5-6,8]</sup>. Still, the cooling curve obtained with UV-VIS spectroscopy is similar to that of the methylated BTAs. This observation hints that the ease of stack formation (i.e. the fraction polymerized material) is similar to the well known polymerization mechanisms which can be predicted by nucleated self-assembly models of the Oosawa and Kasai type<sup>[9,10,11]</sup>. Since the temperature dependent data from CD is not superimposable on the temperature dependent UV-VIS data, one may perceive that the expression of chirality on a supramolecular scale follows a different mechanism. For methylated BTAs, one can argue that only one helix type is formed, but for the D-BTAs a dynamic equilibrium may exist between the two helical senses. The net helicity as function of temperature for D-BTAs cannot be predicted by the modified Oosawa and Kasai nucleated self-assembly model<sup>[4,10,11]</sup>.



**Scheme 1:** Chemical structures of various achiral BTAs and chiral deuterated BTAs

This motivates us to have a closer look at the cooling curve obtained in a dilute solution of dodecane. By a variant of the model

Secondly, the D-BTA showed no Cotton effect at room temperature in cyclic or branched aliphatic solvents, such as respectively MCH or iso-octane (Figure 2). Since this effects is still poorly understood, several experiments were conducted to get more insights in the effect of solvent. For this purpose, we will have a closer look at the cooling curve obtained in a heptane solution. To investigate the effect of solvent composition, solutions in solvent mixtures are investigated with circular dichroism (CD) and UV-VIS spectroscopy. Finally, calorimetric techniques are used to study the self-assembly of BTAs in helical stacks in solution. This technique has already proven itself for studying supramolecular self-assembly, as is shown by Bouteiller *et al*<sup>[12]</sup>. Since D-BTA molecules are very precious, we conduct the calorimetric measurements with an achiral C<sub>16</sub>-BTA (Scheme 1), which is believed to be one of the best soluble BTAs available. This makes it ideal for testing and optimization of this technique.

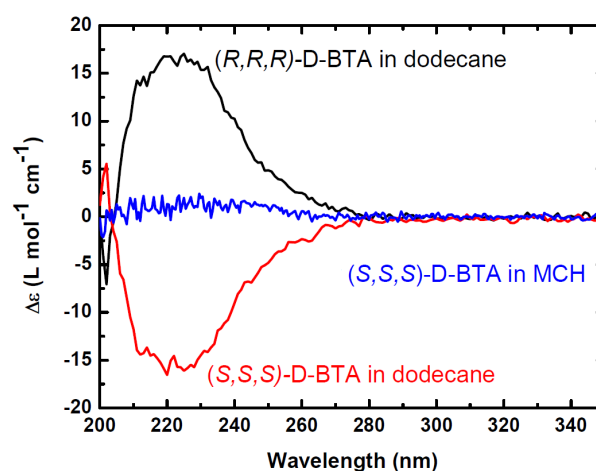


**Figure 2.** CD spectra for D-BTA compounds in various solvents at 20 °C ( $c = 5 \times 10^{-5}$  M).

## Results and Discussion

**Expression of chirality in dodecane.** Cooling curves were obtained with UV-VIS and CD spectroscopy in a dilute solution of the D-BTA in dodecane at a concentration of  $5 \times 10^{-5}$  M by monitoring respectively the optical density (O.D.) and CD effect at 223 nm. We also obtained a cooling curves at a higher concentration ( $c = 4 \times 10^{-4}$  M) and this is included in the Supporting Information. The difference with low concentration is that the curve is shifted to the left, such that a minimum in CD effect is observed at low temperatures. This observation will be discussed in more detail later on. Furthermore, we could not detect the polymerization temperature ( $T_p$ ) for the high concentration, since it is close to the low boiling point of dodecane.

By using a competing nucleated self-assembly model (Figure 1), we hope to get more insights in the obtained cooling curves. For details, we refer to the Supporting Information. Parameters in our model, which are introduced in a natural way out of general principles, are the enthalpy of elongation for active species  $P$  ( $h_{e,P}^*$ ), representing a  $P$ -helix and similarly defined for a active species  $M$  ( $h_{e,M}^*$ ). This designation can be done, since it is known that a negative Cotton effect corresponds to a  $M$ -helix<sup>[5]</sup>. In the model we left this designation open, to make it as general as possible (by indicating active species with  $A$  and  $B$ ). Furthermore, we have the ratio of elongation constants between  $P$  and  $M$  indicated by  $\kappa_{PM}^*$ , and the activation constant  $K_a^*$ , which is assumed to be equal for the  $P$ - and  $M$ -helices. In all cases the asterisk in the parameters indicate that the value is defined at the polymerization temperature  $T_p$ .

Two different fits were done by using this model. To obtain a net helicity  $\langle \theta \rangle$ , the CD spectroscopy data is normalized accordingly. In the first case, the highest CD effect is normed to 0.35 and in the second case it is normed on one. The first normalization choice is motivated by experiments in which a methylated BTA is added to a solution of D-BTAs<sup>[8]</sup>. In both cases the O.D. was normalized to one, to obtain the fraction polymerized material  $\eta$ . The fit results are shown in Table 1 and in Figure 3 only for the second case. The fits for the first case can be found in the Supporting Information (Figure S2).

**Table 1:** Thermodynamic parameters of (*S,S,S*)-D-BTA ( $c = 5 \times 10^{-5}$  M in dodecane,  $T_p=352$  K) obtained by fitting the temperature dependent data.  $M$  is preferred structure.

Norm $\langle \theta \rangle$	$h_{e,M}^*$ (kJ/mol)	$h_{e,M}^* - h_{e,P}^*$ (J/mol)	$K_a^*$ (-)	$-\log_{10} \kappa_{PM}^*$ (-)
<b>0.35</b>	61±3	17±6	(7±1)·10 <sup>-4</sup>	0.0014±0.003
<b>1.00</b>	72±3	(1.7±0.3)·10 <sup>2</sup>	(7±1)·10 <sup>-4</sup>	0.0035±0.0005

In these fits, we see that no good fit could be obtained for the CD normalization at 0.35, while good fits were obtained simultaneously for the UV-VIS and CD data if both are normalized to unity. As is reflected in the small enthalpy differences (which is much smaller than the unit of  $k_B T$ ) and in the small differences of the elongation constants at  $T_p$ , we conclude that small effects can add up to large scale mesoscopic or even macroscopic effects, such as a net helicity. Furthermore, from the fit parameters, we observe that using this model results in a slightly higher cooperativity constant, as compared with a fit from the Van der Schoot model for the achiral  $C_8$ -BTA<sup>[5]</sup>, for which a value of  $2 \times 10^{-4}$  is found. As expected, the enthalpies of elongation  $h_{e,M}^*$  and  $h_{e,P}^*$  are in the same range as obtained for the  $C_8$ -BTA obtained with a variant of the Oosawa and Kasai model. Also, it is observed that no perfect UV-VIS fit is possible. This can be explained by the fact that it is hard to

correct for the non-linear baseline in UV-VIS measurements, which is believed to be present due to optical effects.

Although the quality of the fits from Figure 3 is good, the theoretical prediction for the net helicity in the low temperature regime is less good. There appears to be a small maximum, which is more clear when a higher concentration is used. This effect is observed in heptane as well. A better investigation of this observed phenomenon can be done in heptane, since the melting point of heptane is lower than that of dodecane. This allows us to go to lower temperatures.

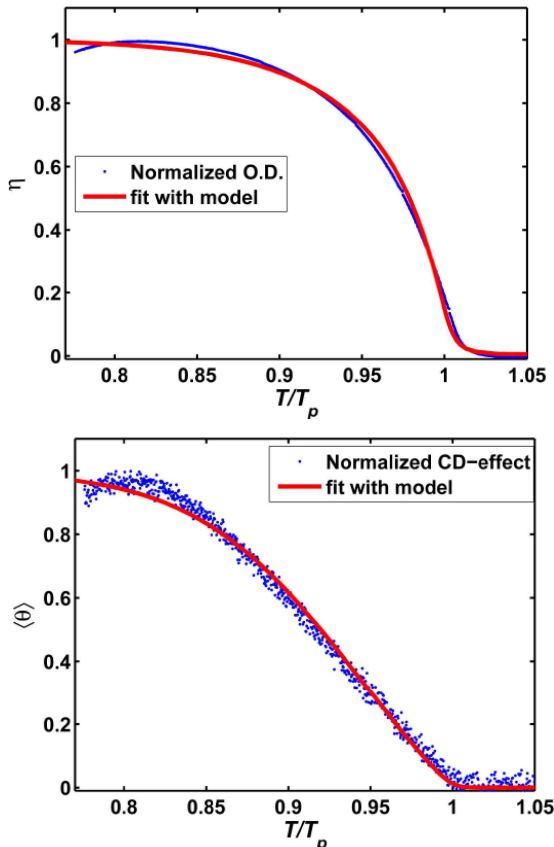


**Figure 3.** Simultaneous fits obtained by normalization of CD effect (net helicity) and O.D. (fraction polymerized material) on one as probed at 223 nm. Fitted experimental data is from a dodecane solution ( $c = 5 \times 10^{-5}$  M) of the (*S,S,S*)-D-BTA.

**Low temperature behavior in heptane.** A cooling curve probed at 223 nm of (*S,S,S*)-D-BTA in heptane is measured at a concentration of  $5 \cdot 10^{-5}$  M. The solution is cooled down to the limits of the temperature controller ( $-10^\circ\text{C}$ ). The result is shown in Figure 2a and in Figure S4. In the low temperature regime an extra extremum is observed in the CD effect, apart from the one that was also observed in dodecane. These two extrema are not observed in the cooling curves obtained from UV-VIS spectroscopy (see Supporting Information). Furthermore, these extrema cannot be predicted by the competing nucleated self-assembly model that is proposed earlier.

To get more information about this observation, the CD spectra for various temperatures were monitored. It was discovered that the shape of the Cotton effect gradually changes in the vicinity of the low temperature extremum (Figure 4(b)-(d)).

The two observed shapes of the Cotton effects are very similar to those observed in methylated BTAs<sup>[5,6]</sup>. The same shape of the CD spectra at high temperatures for the D-BTA are measured for methylated BTAs with the methyl substituted on an odd position in the alkyl chain. In contrast, the Cotton effect at low temperatures is similar to the Cotton effect measured for methylated BTAs on an even position<sup>[6]</sup>. This odd-even effect that is observed in methylated

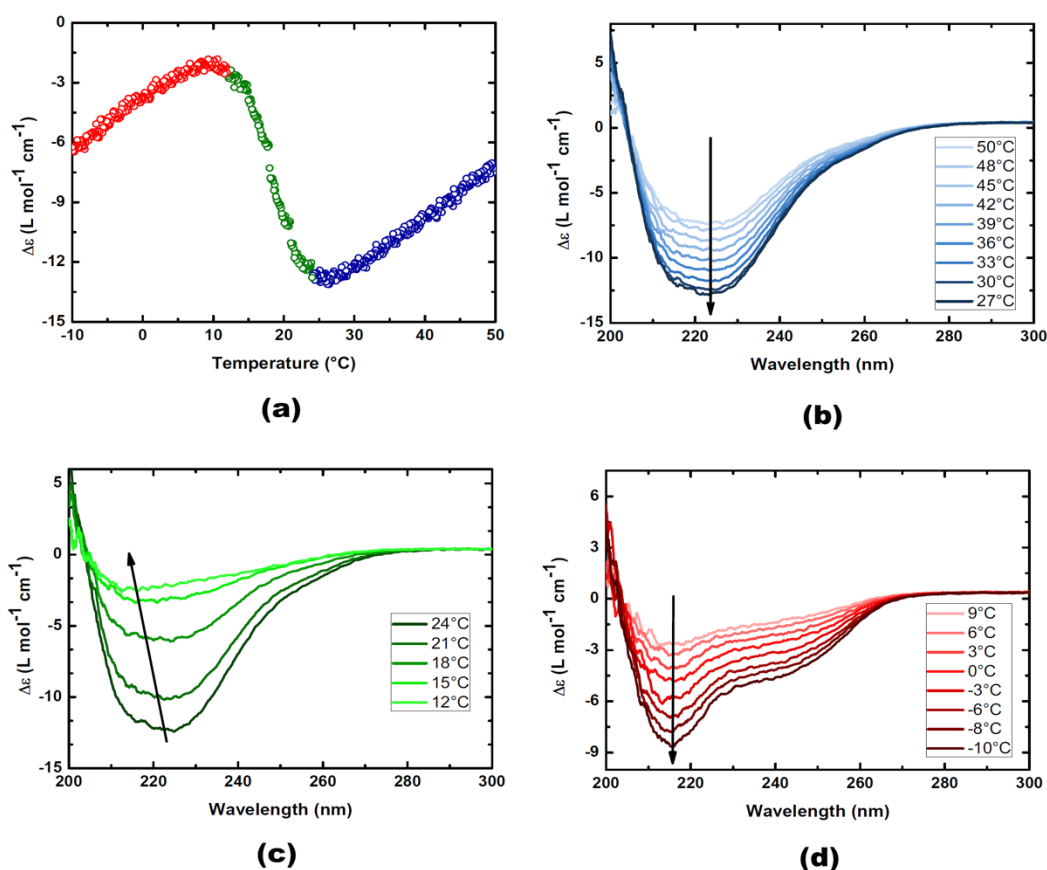


**Figure 4.** (a) Cooling curve obtained for the (S,S,S)-D-BTA in heptane ( $c = 5 \times 10^{-5}$  M) by probing the CD effect at 223 nm. Colors indicating various temperature regimes (b)-(d) Detailed shapes of the Cotton effects as function of temperature for the various temperature regimes. Arrows indicate cooling.

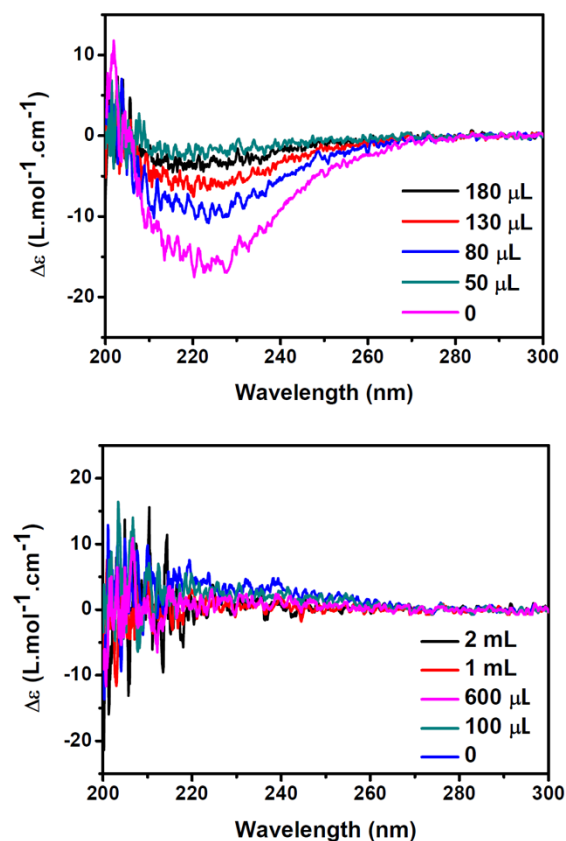


**Figure 5.** CD spectra of titration experiments conducted at room temperature (20 °C). To a 2 mL solution of (S,S,S)-D-BTA in heptane ( $c = 5 \times 10^{-5}$  M) MCH is added (top) and to a 2 mL solution of (S,S,S)-D-BTA in MCH ( $c = 5 \times 10^{-5}$  M) the effect of heptane addition is shown (bottom). The volume of solvent added is shown in the insets.

BTAs is thus similar to the change of the Cotton effect for D-BTAs. The difference however is that this effect is now induced by temperature. So in the case of D-BTAs, we cannot really speak about an odd-even effect and for this reason we call it an odd-even like effect.

Odd-even effects are usually observed in the macroscopic ordering of molecules, such as in liquid crystals. For example, the length of an alkyl chain influences the transition temperature from one liquid crystalline phase to another in an oscillatory fashion<sup>[13]</sup>. Furthermore, it is shown that whether the length of this chain is odd or even, determines the helical sense of cholesteric phases (if present). Since now an odd-even like effect is observed in quasi-one dimensional stacks, we can hypothesize that the solvent may play an active role in the self-assembly process.

Finally, we remark that the odd-even effect in methylated BTAs is both in shape and sign, while for D-BTAs in heptane the odd-even like effect seems to be only in shape. However, if we add a cyclic or branched solvent to the solution, we shall see in the next section that the sign of the Cotton effect can be inverted at certain temperatures. Furthermore, notice that care needs to be taken while interpreting Figure 4(a), since it is not corrected for the wavelength change of the maximal CD effect. However, this effect is small, since the overall shape will be the same if this correction would be done.

**Influence of solvent composition on the helical stacking of D-BTAs.** To get a better understanding of the role of solvent in the self-assembly process, a D-BTA solution in a solvent in which a Cotton effect seems to be absent is considered (MCH) and in which it is present (heptane). Adding MCH to a solution in heptane, reduces the Cotton effect at room temperature, as can be seen in Figure 5 (top). However, adding pure heptane to a solution in MCH (up to a v/v of 50%), no Cotton effect is observed at room temperature (Figure 5 (bottom)). To further investigate this latter observation, the cooling curves for various solvent compositions were measured at 223 nm, keeping the concentration of D-BTA constant at  $c = 5 \cdot 10^{-5}$  M. The result is shown in Figure 6 (top).

A comparison of the different cooling curves obtained by this experiment, gives rise to temperature regimes where all curves overlap. It still remains an open question why this is observed. Also, it is observed that a positive, but small Cotton effect can be



measured, starting from a certain amount of MCH added. As an example, we included the CD spectrum for a MCH volume fraction of 0.29 at  $T = 40\text{ }^{\circ}\text{C}$  in Figure 6 (bottom).

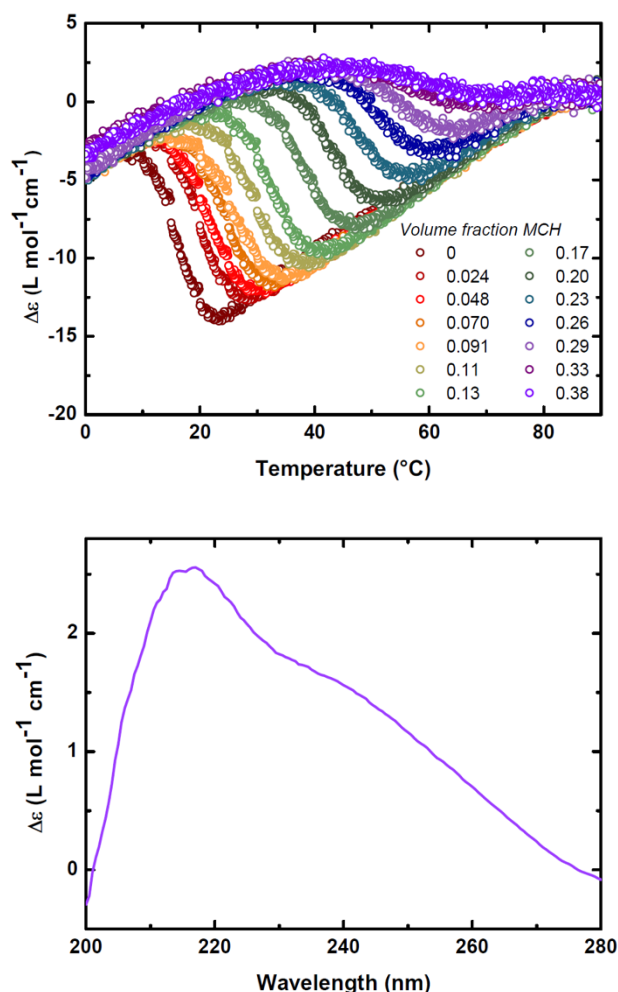


**Figure 6.** Cooling curves obtained from the CD spectra at 223 nm for (*S,S,S*)-D-BTA in a solution of heptane and MCH (top). MCH volume fractions are shown in inset. A positive Cotton effect is observed at a MCH volume fraction of 0.29 at a temperature of  $40\text{ }^{\circ}\text{C}$  (bottom).

The same titration experiments are also conducted with a branched alkane (iso-octane), since also for this solvent, no Cotton effect could be observed at room temperature. The results are the same as in the case of MCH, with the difference that larger amounts of iso-octane are needed to obtain a similar result obtained with MCH. Furthermore, again a positive effect could be observed in iso-octane (see Supporting Information).

Following the same arguments as Stals *et al.* for the methylated BTAs, two different Cotton effects imply two different helical packings<sup>[6]</sup>. However, for methylated BTAs this can be attributed purely to steric reasons, but this is not possible with deuterated BTAs. Still, we can hypothesize that there might be a competition of binding of solvent to the growing aggregate and that the conformation of the helix is influenced by the amount and type of solvent attached to it. That this could be possible, is reflected in the different observations made between the MCH and iso-octane titration experiments.

**Heat capacity measurements to study self-assembly of BTAs.** Heat capacity measurements are of interest to study the self-assembly in supramolecular assemblies, since every transition similar to a phase transition results in a peak of the heat capacity. The shape of the peak gives information about the type of transition and this will hopefully lead to more insights for the D-BTA system. As an extra, this technique will also supply thermodynamic data, which up until now is often obtained by fitting cooling curves with theoretical models such as the nucleated self-assembly model of Van der Schoot.

To measure the enthalpy releases in (dilute) solution, a very sensitive technique is needed. During this project, a microDSC was used for this purpose. The difficulty with this device is that only small heating/cooling rates can be obtained ( $< 1\text{ K/min}$ ), which makes it hard to fully optimize the temperature programme. Cooling is in this case more difficult than heating, since a fan is used in order to get sufficiently slow cooling. This fan may induce noise in the obtained thermogram. These disadvantages are troublesome, but it allows this technique to be very sensitive, which makes it interesting for studying self-assembly in solution. Our goal is to do calorimetric measurements at concentrations as low as possible. Preferably, concentration in the  $10^{-5}\text{ M}$  range need to be measured, such that comparisons are possible with spectroscopic data (UV-VIS and CD).

The achiral- $\text{C}_{16}$ -BTA is used in order to test this experimental technique. The results of a heating run ( $0.1\text{ K/min}$ ) for concentrations 0.1 mg/ml and 1 mg/ml in dodecane are shown in Figure 7.

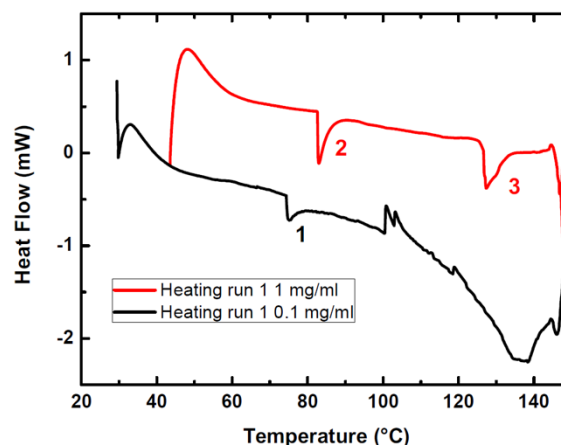


**Figure 7.** Heat traces for the achiral- $\text{C}_{16}$ -BTA in dodecane in two different concentrations. Peaks of interest are indicated with numbers.

As can be seen, two peaks in the heating flow (which is proportional to the heat capacity) are seen for 1 mg/ml, while only one peak is observed in the 0.1 mg/ml sample. The rest of the heating trace is presumed to be noise. These peaks are integrated in order to obtain the enthalpy release and are normalized with respect to the amount of BTA monomeric units present in solution. The results are shown in Table 2.

**Table 2:** Thermodynamic data of the achiral- $\text{C}_{16}$ -BTA obtained by microDSC measurements.

Concentration (mg/ml)	Peak number	Temperature ( $^{\circ}\text{C}$ )	$\Delta H$ (kJ/mol)
0.1	1	74	588
1.0	2	83	84
1.0	3	127	65

## Experimental Section

As we compare the obtained  $\Delta H$  values with the fits obtained from UV-VIS data with the model of Van der Schoot, we discover that peak 3 is remarkably close to the value of the enthalpy of elongation  $h_e$  of the achiral  $C_8$ -BTA, for which a value of -69 kJ/mol is found<sup>[5]</sup>. However, it is unknown what transition is measured in peak 2. This transition is not seen in spectroscopic measurements in dilute solution. Furthermore, the  $\Delta H$  value of peak 1 is a factor 10 off for what we would obtain by a fit. This indicates that the signal in the 0.1 mg/ml sample should be questioned.

These observations show that we can obtain results for concentrations as low as 1 mg/ml ( $\sim 10^{-3}$  M), but it also shows that the technique still needs optimization. One flaw is that in subsequent cooling runs and heating runs, no peaks in the heat flow are observed, meaning that the measurements are not reproducible in the same temperature programme (Figure S8). This needs more investigation. Furthermore, it is observed in these measurements that the device has problems to reach the temperature set in the programme for the cooling curve, since only low cooling rates can be attained. Still, the shape of the peaks in heat capacity are expected for transitions similar to thermodynamic phase transitions.

## Conclusion

Deuterated benzene-1,3,5-tricarboxamides were investigated with CD spectroscopy and UV-VIS spectroscopy in dilute solution. For this system it is observed that the solvent plays an important role in the self-assembly process, as is shown in the fact that Cotton effects are not displayed in all solvents at room temperature. Theoretical modelling showed that experimental data from these experimental techniques could be predicted by considering a competition in formation between two active species. However, we had to normalize CD and UV-VIS data both on unity to obtain good results. These fits showed that small energy differences, much less than the order of  $k_B T$ , can result in macroscopic observables, such as a net helicity.

A detailed look at the cooling curve in heptane, showed us that it can be hypothesized that solvent plays an active role in the self-assembly process in a length scale larger than that of an aggregate. Solvent mixing experiments showed that we could even infer a competition of binding of solvent molecules to the aggregate, which alters the helical packing of the stacks. Finally, micro-DSC was tested as a technique to study supramolecular self-assembly in solution. Although the technique is promising, it still needs some optimization and thorough testing.

In order to get more insights in the active role of solvent for D-BTAs, vibrational circular dichroism (VCD) measurements will be conducted in the near future. This technique may give insightful new information in the hydrogen bonding in a chiral environment. Furthermore, we advise to have a look at lower temperatures in heptane than -10°C with CD spectroscopy. Finally, at the moment the  $\beta$ -substituted D-BTA is investigated in dilute solution. However in this case, no odd-even effect as in the methylated BTAs was observed.

**Materials:** Heptane, dodecane, iso-octane and methylecyclohexane were obtained from Acros in spectroscopic grade and used as received. Benzene-1,3,5-tricarboxamides were synthesized and characterized in accordance with published procedures<sup>[6,7]</sup>.

**Methods:** UV-vis and Circular Dichroism measurements were performed on a Jasco J-815 spectropolarimeter where the sensitivity, time constant and scan rate were chosen appropriately. Corresponding temperature-dependent measurements were performed with a PFD-425S/15 Peltier-type temperature controller with a temperature range of 263-383 K and adjustable temperature slope, in all cases a temperature slope of 1 K/min was used. In all other measurements the temperature was set at 20 °C. In all experiments the linear dichroism was also measured and in all cases no linear dichroism was observed. Solutions were prepared by weighing in the necessary amount of compound for a given concentration, where after this amount was transferred to a volumetric flask. Then the flask was filled for  $\frac{3}{4}$  with the spectroscopic grade solvent and put in an oscillation bath at 40 °C for 45 minutes, whereafter the flask was allowed to cool down and filled up to its meniscus. The  $\Delta \epsilon$  value is calculated with the expression  $\Delta \epsilon = CD \text{ effect}/(32980 \cdot c \cdot l)$  where  $c$  is the concentration in mol/L and  $l$  is the optical path length in cm. The thermal transitions were determined with microDSC using a Setatram C80-II Calvet microcalorimeter with heating and cooling rates of 0.4 K/min.

## Acknowledgements

The authors would like to thank Maarten Smulders for his help with the experimental work and the insightful discussions. The help of Hugo Meekes and Jacques van Eupen with the micro-DSC measurements is also greatly appreciated. The following people are thanked for their discussions on this topic: Patrick Stals, Tom de Greef, Marko Nieuwenhuizen, Leon van Dijk, Jef Vekemans and Bert Meijer.

- 
- [1] J.H. van 't Hoff, *Arch. Neerl. Sci. Exactes Nat.* **1874**, 9, 445-454.
  - [2] B. Alberts, A. Johnson, J. Lewis, M. Raff, K. Roberts, P. Walter, *Molecular Biology*, 5th edition, (Garland Science, New York **2008**).
  - [3] K. Cheon, M.M. Green, *J. Label. Compd. Radiopharm.* **2007**, 50, 961-966
  - [4] P. Jonkheijm, P. van der Schoot, A.P.J.H. Schenning, E.W. Meijer, *Science* **2006**, 313, 80-83.
  - [5] M.M.J. Smulders, *Chirality in Supramolecular Polymers*, PhD Thesis, Eindhoven University of Technology, **2009**.
  - [6] P.J.M. Stals, M.M.J. Smulders, R. Martin-Rapun, A.R.A. Palmans, E.W. Meijer, *Chem. Eur. J.* **2009**, 15, 2071-2080.
  - [7] D.W.R. Balkenende, S.Cantekin, C. Duxbury, M.H.P. van Genderen, A.R.A. Palmans, E.W. Meijer, Manuscript in preparation.
  - [8] S. Cantekin, D.W.R. Balkenende, M.M.J. Smulders, A.R.A. Palmans, E.W. Meijer, Manuscript in preparation.
  - [9] F. Oosawa, M. Kasai, *J. Mol. Biol.* **1962**, 4, 10-21.
  - [10] P. van der Schoot, *Theory of Supramolecular Polymerization* In: *Supramolecular Polymers* (Ed.: A. Ciferri), 2nd edition, (Taylor and Francis, London, **2005**).
  - [11] P. van der Schoot, *Nucleation and Co-Operativity in Supramolecular Polymers* In: *Advances In Chemical Engineering Volume 35*, Academic Press, **2009**.
  - [12] L. Bouteiller, *Adv. Polym. Sci.* **2007**, 207, 79-112.
  - [13] a) W. H. de Jeu and J. van der Veen, *Mol. Cryst. Liq. Cryst.* **1977**, 40, 1-17. b) G. W. Gray and D. G. McDonnel, *Mol. Cryst. Liq. Cryst.* **1977**, 34, 211-217. c) D. Demus in *Handbook of Liquid Crystals Volume 1: Fundamentals* (Eds.: D. Demus, J. Goodby, G. W. Gray, H.-W. Spiess and V. Vill), Wiley-VCH Weinheim **1998**, Chapter VI, pp. 146-152. d) J. W. Goodby in *Handbook of Liquid Crystals Volume 1: Fundamentals* (Eds.: D. Demus, J. Goodby, G. W. Gray, H.-W. Spiess and V. Vill), Wiley-VCH Weinheim **1998**, Chapter V, pp. 124-126.
-

**Supporting Information for:**

**Expression of chirality in deuterated benzenetricarboxamides**

*Jeffrey C. Everts, Seda Cantekin, Paul van der Schoot, Anja R. A. Palmans*

**Table of Contents:**

Competing nucleated self-assembly model	8
Supporting Figures	12
References	19

## Competing nucleated self-assembly model

In order to describe the experimental data obtained from the D-BTAs a nucleated self-assembly model was derived by an extension of the Oosawa and Kasai model<sup>[1]</sup> that takes into account a competition between the formation of two types of aggregates. We have chosen a version that is not self-catalyzed, since it is reasonable to assume that every monomeric unit needs to undergo a conformational change in order to attach to a growing polymer chain. Such a conformational change can be imagined by tilting of the amide moieties in a BTA molecule such that it can accommodate hydrogen bonding with other monomeric units in a stack. Notice however that no difference is seen if we had chosen a self-catalyzed version of this model<sup>[2]</sup>. Since the derivation of the model is rather extensive, we have reported the calculations elsewhere<sup>[3]</sup>. Only the most important steps will be mentioned, with some intermediate results.

The system that we will consider here consists of inactive species  $i$  and two active species, which we call  $A$  and  $B$ . An active species could be a  $P$ - or a  $M$ -helix. Since we want to make this model as general as possible, we do not make any specifications yet. In a saddle point approximation we can set the free energy as follows:

$$\frac{\beta f_i}{V} = \underbrace{\rho_i \ln(\rho_i v) - \rho_i}_{\text{ideal mixing entropy}} - \underbrace{\rho_i \ln Z_i}_{\text{single particle free energy}} \quad (1)$$

$$\frac{\beta f_\alpha}{V} = \sum_{N=1}^{\infty} \underbrace{\rho_\alpha(N)}_{\text{size distribution}} \left[ \underbrace{\ln(\rho_\alpha(N)v) - 1}_{\text{ideal mixing entropy}} - \underbrace{N \ln Z_\alpha}_{\text{free energy of monomers in aggregate}} + \underbrace{\beta G_\alpha(N-1)}_{\text{free energy of binding}} \right] \quad (\alpha = A, B) \quad (2)$$

Here,  $\beta := 1/k_B T$ , with  $k_B$  the Boltzmann constant and  $T$  the absolute temperature,  $V$  is the system volume,  $\rho_k$  indicate the various number densities ( $k=i, A, B$ ),  $v$  is the volume of a solvent molecule,  $Z_k$  are partition functions of the monomers in species  $k=i, A, B$  and  $G_\alpha$  is a free energy of binding for  $\alpha = A, B$ . By doing a functional minimalization of the total free energy ( $f = f_i + f_A + f_B$ ), with respect to conservation of mass, equilibrium size distributions are obtained.

Furthermore, we obtain a mass action law after extensive algebraic manipulations.

$$\phi K = \underbrace{1 - \frac{1}{\bar{N}_A}}_{\text{monomers}} + \underbrace{K_a \bar{N}_A (\bar{N}_A - 1)}_{\text{polymers type A}} + \underbrace{K_a \left( \frac{\bar{N}_B}{\bar{N}_A} \right)^2 \bar{N}_A (\bar{N}_A - 1)}_{\text{polymers type B}} \quad (3)$$

Here,  $\phi$  is a total mole fraction defined as the sum of mole fractions of species  $i, A$  and  $B$ . This quantity can be seen as the probability of a certain species to be in the vicinity of a growing aggregate which is amplified by a gain of free energy as is expressed in the equilibrium constant  $K$ . The product  $\phi K$  can thus



be seen as a measure for the probability of a molecule attaching to an aggregate. In (3),  $K$  is the product of the activation constant  $K_a$ , that regulates the equilibrium between inactive and active species, and an elongation constant  $K_{e,A}$ , that regulates the growth of active species  $A$ . The fact that  $K$  is defined in this manner is reflected by the non-selfcatalyzed nature of the model.

Furthermore, we have chosen to parametrize our problem with the aggregation number of species  $A$ ,  $\bar{N}_A$ , which is similarly defined for species  $B$ , to make the competition between  $A$  and  $B$  explicit. The following relation can be found for the ratio of aggregation numbers of species  $A$  and  $B$ .

$$\frac{\bar{N}_A}{\bar{N}_B} = \bar{N}_A - \kappa_{BA}(\bar{N}_A - 1) \geq 0 \quad (4)$$

Here  $\kappa_{BA} := K_{e,B} / K_{e,A}$ , a ratio of elongation constants. If we let  $\kappa_{BA} \rightarrow 0$ , we obtain the mass action law of a system with only one active species<sup>[2,3]</sup>. Notice also that by our choice of parametrization, the model looks asymmetric. This is a small price we have to pay to make the competition between  $A$  and  $B$  explicit, since another (probably less convenient) choice of parametrization could leave the symmetry between  $A$  and  $B$  intact. Now we can imagine the following scheme by this model (repeat of Figure 1).

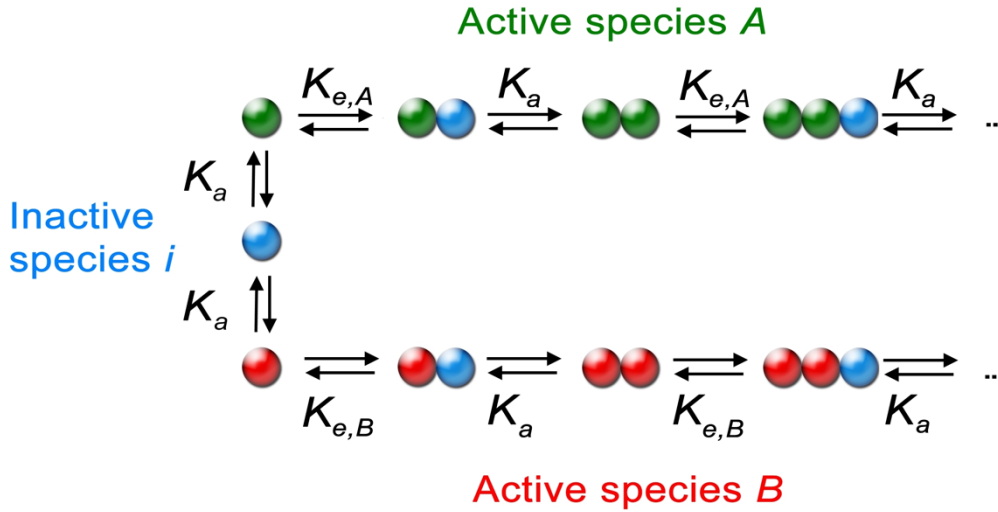


Figure S-1. Scheme for competing nucleated self-assembly model

By using mass action law (3), expressions can be obtained for the net helicity and fraction polymerized material. This can be done easily since we can distinguish three different contributions which are proportional to the mole fractions of inactive species  $i$  ( $\phi_i$ ) and the active species  $A$  and  $B$  ( $\phi_A$  and  $\phi_B$ ).

We define the net helicity  $\langle \theta \rangle$  as:

$$\langle \theta \rangle = \frac{\phi_A - \phi_B}{\phi_i + \sum_{\alpha=A,B} \phi_\alpha} \quad (5)$$

Observe that we include the inactive species in the normalization. This is done since the CD effect is proportional to the net helicity. This condition will be satisfied by the choice of this definition, since  $\phi$  is a conserved quantity.

The fraction polymerized material  $\eta$  can be defined using the following equation:

$$\eta = \frac{\phi_A + \phi_B}{\phi_i + \sum_{\alpha=A,B} \phi_\alpha} \quad (6)$$

An arbitrary equilibrium constant  $K'$  is a Boltzmann weighed factor of a free energy of binding  $g$  by  $K' = \exp(-\beta g)$ , meaning that we can introduce temperature dependency by Taylor expansion. This makes it possible to find analytical expressions for the net helicity and fraction polymerized material as function of temperature by using the mass action law<sup>[3]</sup>. However, the expression for the net helicity becomes less accurate in the low temperature regime. For this reason, the equations are solved numerically by a fixed point like method. The only constraint for this choice is that the activation constant cannot be temperature dependent. However, no problems are expected by this constraint. We have chosen to expand all equilibrium constants ( $K_{e,A}$  and  $K_{e,B}$ ) to first order, while  $K_a$  is expanded to zeroth order, both around the polymerization temperature  $T_p$ . By doing this, an enthalpy of elongation is introduced for both active species ( $h_{e,A}^*$  and  $h_{e,B}^*$ ), an activation constant  $K_a^*$  and a ratio of elongation constants  $\kappa_{BA}^* := K_{e,B}^* / K_{e,A}^*$ . The asterisk here denotes that these quantities are defined at  $T_p$ . The following MATLAB script is used to fit experimental data by simulation of this procedure.

```
%MATLAB script for fitting temperature dependent CD and UV-VIS spectroscopy
%data by simulation of the competing nucleated self-assembly model.

close all;
clear all;

%Defining constants

% parameters for normalized on one kantelen
heB = -20.95;
heA = -21;
Ka = 7.5*10^-4;
KBA = 10^-0.0038;
M = 20000;           %maximum aggregation number
Tp = 352;

% Load raw data and normalize (this needs to be done manually by the user or by
% already doing this in the ASCII file
load dodecaneraw.txt

T_Te = (dodecaneraw(:,1)+273.15)./Tp;
normcd = (dodecaneraw(:,2)-0.9)./(-20-0.9);
normod = ((1-(dodecaneraw(:,3)-1.7)/(2.16-1.7))-(1*T_Te-1.43)-0.4)*0.82;

%Create list of values

T_Tp= zeros(M,10);

%Starting estimate (aggregation number = i+0.01)
for i = 1:M
    T_Tp(i,1) = 1+(1/heA)*log(1-1/(i+0.01)+2*Ka*(i+0.01)*((i+0.01)-1));
end
```

```

for j = 2:10
    for k = 1:M
        T_Tp(k,j) = 1+(1/heA)*log(1-1/(k+0.01)+Ka*(k+0.01)*((k+0.01)-1)+...
            Ka*((k+0.01)-exp(log(KBA)+(heB-heA)*(T_Tp(k,j-1)-1)))^-2*(k+0.01)*...
            ((k+0.01)-1));
    end
end

% Make list of net helicity as function of Na

theta = zeros(M,1);

for k = 1:M
    theta(k,1) = (Ka*(k+0.01)*((k+0.01)-1)-Ka*(k+0.01)*((k+0.01)-1)*...
        ((k+0.01)-((k+0.01)-1)*exp(log(KBA)+(heB-heA)*(T_Tp(k,10)-1)))^-2)/(1-
        1/(k+0.01)+...
        Ka*(k+0.01)*((k+0.01)-1)+Ka*(k+0.01)*((k+0.01)-1)*...
        ((k+0.01)-((k+0.01)-1)*exp(log(KBA)+(heB-heA)*(T_Tp(k,10)-1)))^-2);
end

for k = 1:M
    eta(k,1) = (Ka*(k+0.01)*((k+0.01)-1)+Ka*(k+0.01)*((k+0.01)-1)*...
        ((k+0.01)-((k+0.01)-1)*exp(log(KBA)+(heB-heA)*(T_Tp(k,10)-1)))^-2)/(1-
        1/(k+0.01)+...
        Ka*(k+0.01)*((k+0.01)-1)+Ka*(k+0.01)*((k+0.01)-1)*...
        ((k+0.01)-((k+0.01)-1)*exp(log(KBA)+(heB-heA)*(T_Tp(k,10)-1)))^-2);
end

figure(1)
hold on
box on
xlim([0.77 1.05]);
ylim([-0.01 1.1]);
set(gca, 'linewidth',1.5, 'FontWeight', 'bold', 'FontSize',14,...
    'FontName', 'Arial');
xlabel('T/T_p', 'FontWeight', 'bold', 'Fontangle', 'italic', 'FontSize',16, 'FontName', 'ari
al');
ylabel('\eta', 'FontWeight', 'bold', 'Fontangle', 'italic', 'FontSize',16, 'FontName', 'aria
l');
plot(T_Te, normod, 'b.', 'LineWidth',3)
plot(T_Tp(:,10), eta, 'r-', 'LineWidth',3)
legend('Normalized O.D.', 'fit with model', 'Location', 'Best')
hold off

figure(2)
hold on
box on
xlim([0.77 1.05]);
ylim([-1 1.1]);
set(gca, 'linewidth',1.5, 'FontWeight', 'bold', 'FontSize',14,...
    'FontName', 'Arial');
xlabel('T/T_p', 'FontWeight', 'bold', 'Fontangle', 'italic', 'FontSize',16, 'FontName', 'ari
al');
ylabel('\langle\theta\rangle', 'FontWeight', 'bold', 'Fontangle', 'italic', 'FontSize',16,
'FontName', 'arial');
plot(T_Te, normcd, 'b.')
plot(T_Tp(:,10), theta, 'r-', 'LineWidth',3)
legend('Normalized CD-effect', 'fit with model', 'Location', 'Best')
hold off

```

## Supporting Figures

Figure S2. The effect of concentration on temperature dependent CD for the (*S,S,S*)-D-BTA compound. Raw data is shown obtained from monitoring the CD effect at 223 nm.

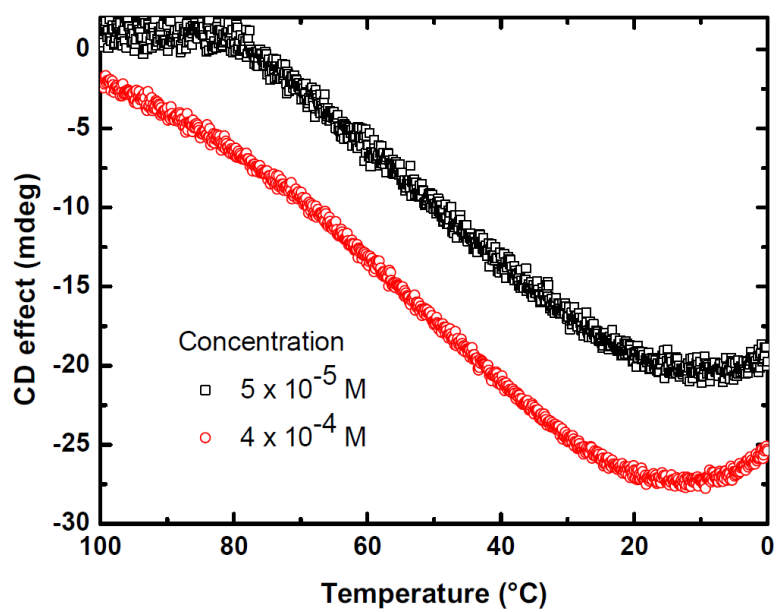


Figure S3. Fits for net helicity  $\langle \theta \rangle$  normalized to 0.35, with simultaneous fit obtained for the fraction polymerized material  $\eta$  normalized to unity.

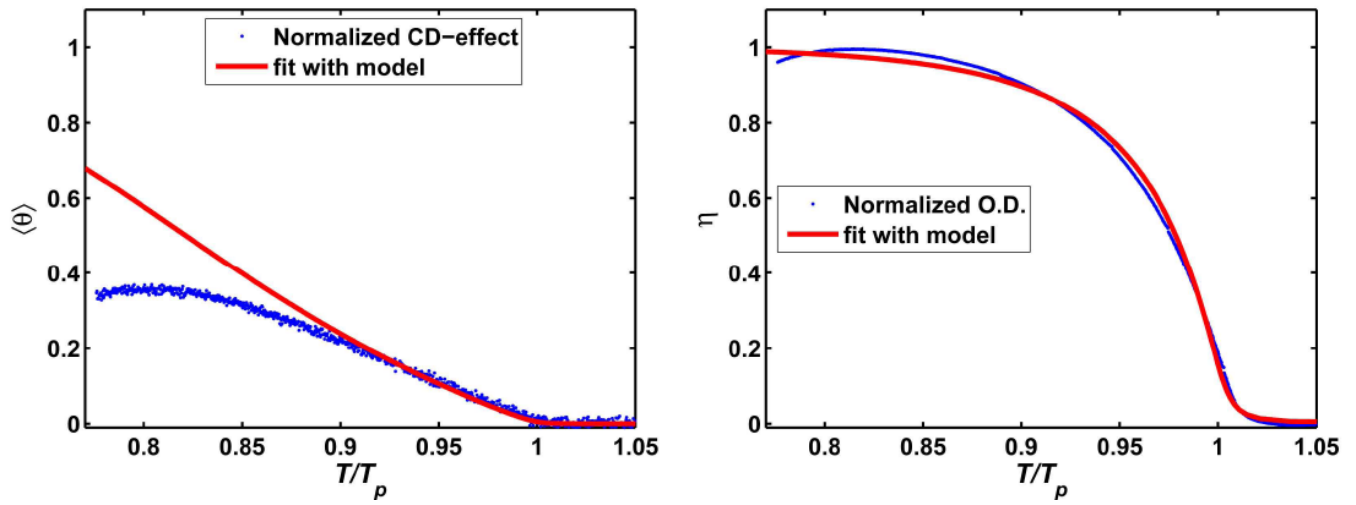
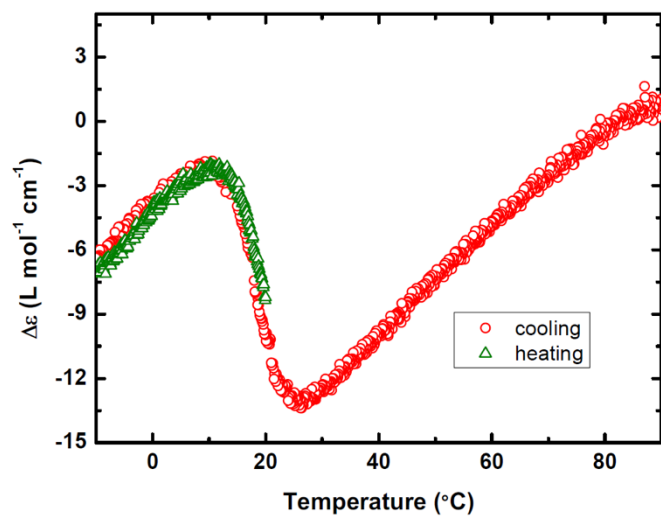
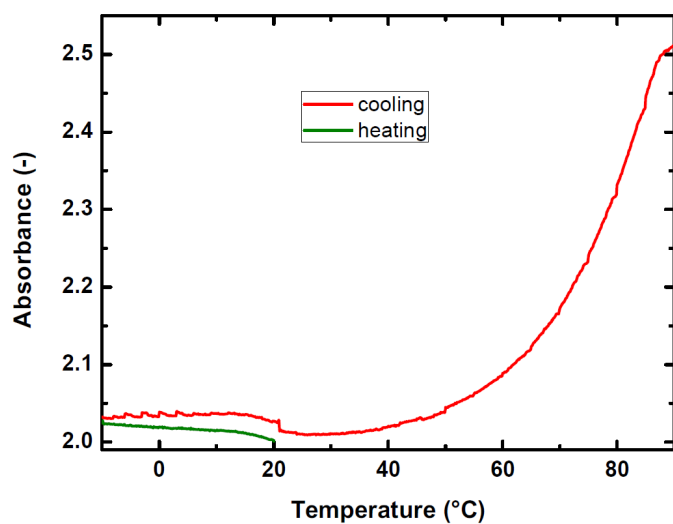


Figure S4. Temperature dependent CD and UV-VIS curves for the (*S,S,S*)-D-BTA compound in heptane ( $c = 5 \times 10^{-5}$  M). For both cases cooling and heating was performed to investigate the presence of hysteresis.



(A)



(B)



Figure S5. Temperature dependent UV-VIS data for the (*S,S,S*)-D-BTA compound in solutions of heptane and MCH (MCH volume fraction shown in inset) for  $c = 5 \times 10^{-5}$  M. O.D. is monitored at 223 nm.

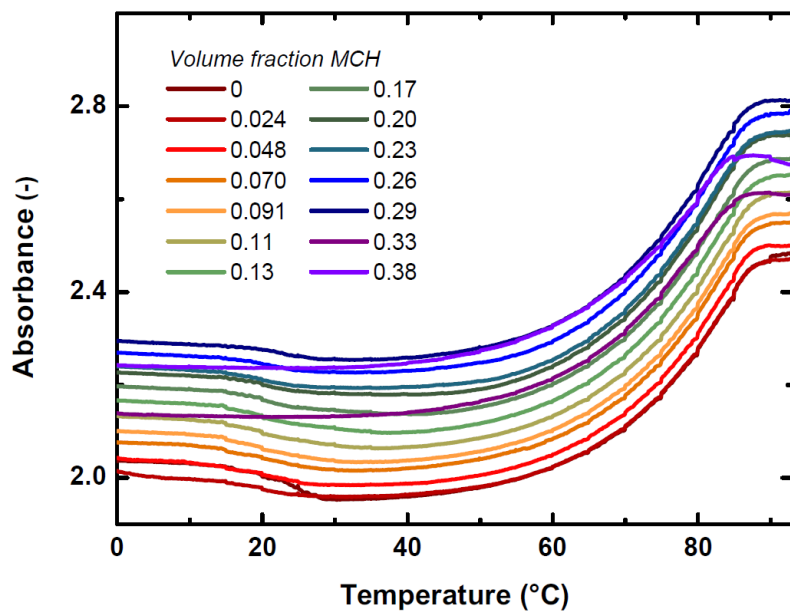
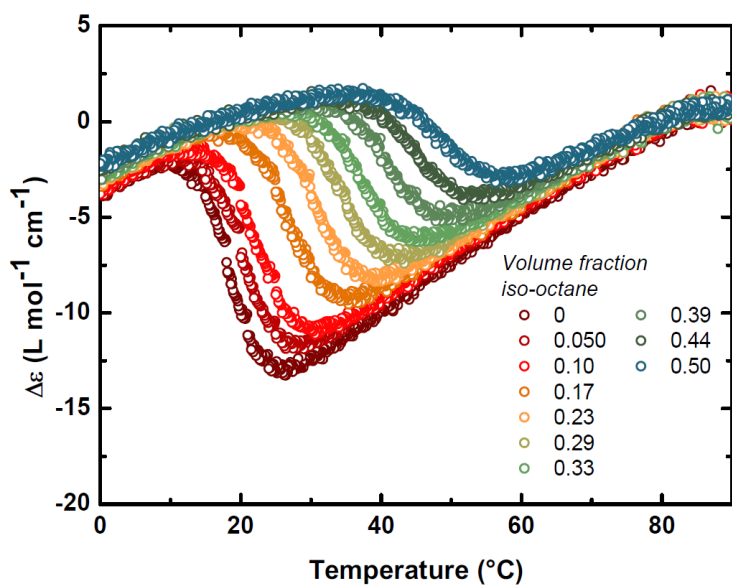
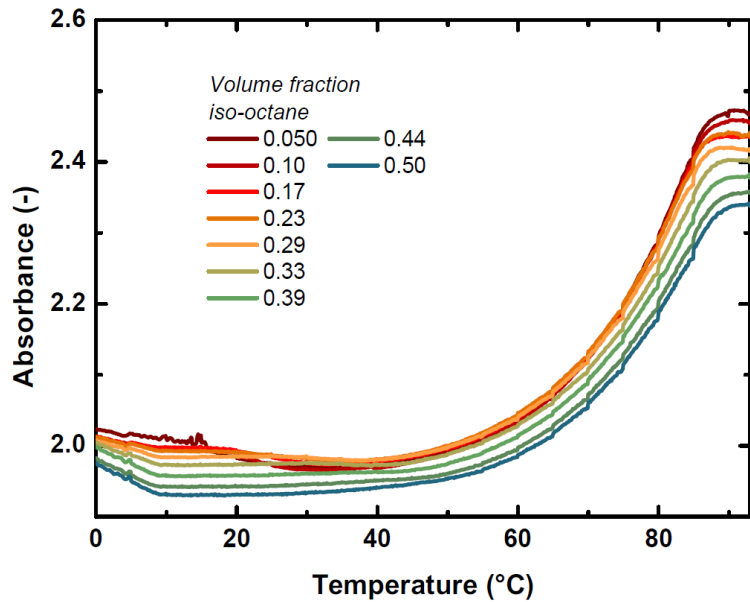


Figure S6. Temperature dependent CD and UV-VIS for various solutions of the (*S,S,S*)-D-BTA in heptane and iso-octane (volume fraction iso-octane shown in inset) for  $c = 5 \times 10^{-5}$  M. Raw data is shown for UV-VIS data. CD and O.D. are both monitored at 223 nm.



(A)



(B)

Figure S7. Positive Cotton effect measured for a (*S,S,S*)-D-BTA solution in iso-octane at 40 °C ( $c = 5 \times 10^{-5}$  M)

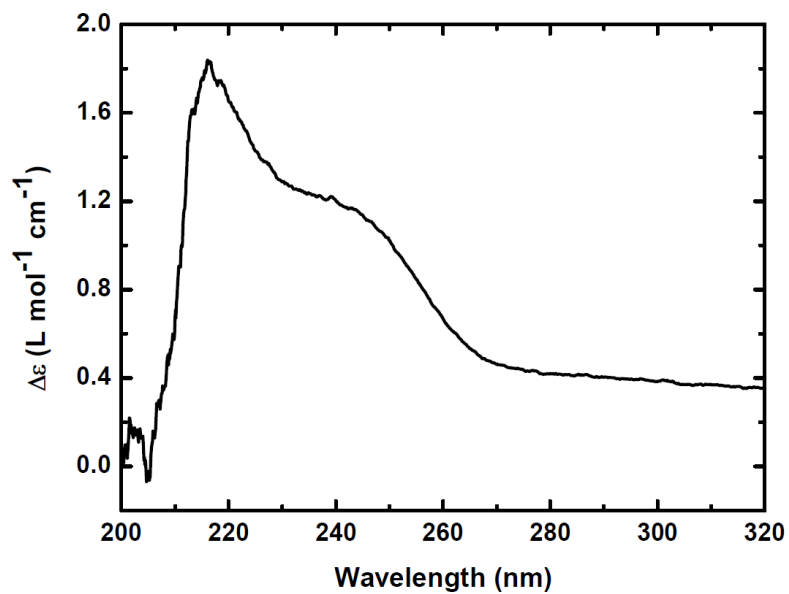
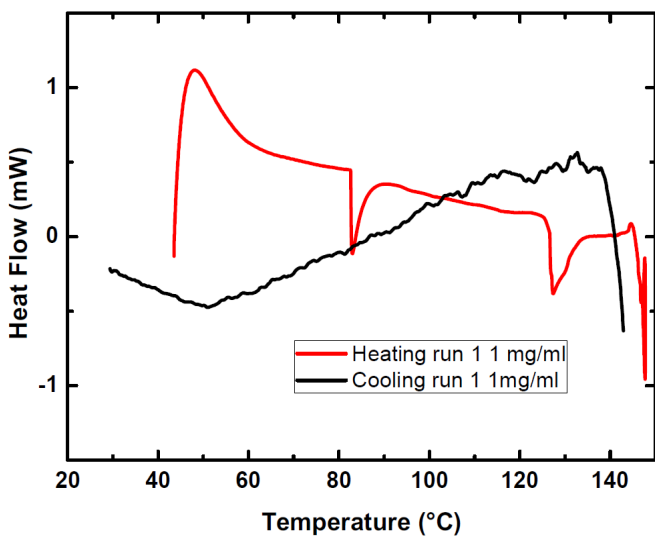
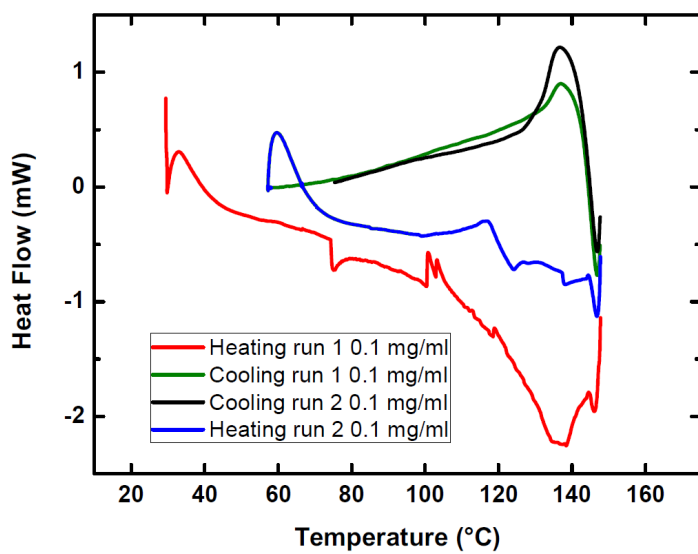


Figure S8. Heating and cooling traces for the achiral- $C_{16}$ -BTA in dodecane for two different concentrations.



(A)



(B)

## References

- [1] F. Oosawa, M. Kasai, *J. Mol. Biol.* **1962**, *4*, 10-21.
- [2] P. van der Schoot, *Nucleation and Co-Operativity in Supramolecular Polymers* In: *Advances In Chemical Engineering Volume 35*, Academic Press, **2009**.
- [3] J.C. Everts, *Expression of chirality by competing nucleated self-assembly*, Internal Internship report, Eindhoven University of Technology, **2010**.